Int. J. Heat Mass Transfer. Vol. 35, No. 1, pp. 131–140, 1992
Printed in Great Britain

0017–9310/92 $5.00 + 0.00

Mean emission length approach to multidimensional radiative transfer including scattering and real gas absorption

D. V. WALTERS† and R. O. BUCKIUS

Department of Mechanical and Industrial Engineering, University of Illinois at Urbana–Champaign, 1206 W. Green Street, Urbana, IL 61801, U.S.A.

(*Received* 25 *July* 1990 *and in final form* 3 *January* 1991)

Abstract—A computational approach to radiative emission analysis is presented for applications where multidimensional, absorbing, emitting, and scattering media are important and real gas contributions must be incorporated. The mean emission length method of solving for the energy transfer is developed as an approximate yet accurate approach to such problems. Although developed using the photon path length method, the resulting analysis does not require knowledge of the photon path length distribution functions. Examples of the application of this approach for emission are included with particular emphasis upon its utility in problems involving real gases and scattering particles. Numerical results for planar and cylindrical media for ranges of optical depth and scattering albedo are presented, and the superior accuracy and computational efficiency of this method as compared to other common approaches are demonstrated.

INTRODUCTION

CHARACTERISTIC lengths for radiative transfer in general multidimensional absorbing, emitting and scattering systems have been developed in a previous study [1], and the importance of such lengths to the general understanding of radiative transfer phenomena is noted. The mean beam length and geometric mean beam length are alternate characteristic lengths which scale complex volumes to a single line-of-sight. These lengths characterize emission from isothermal gas volumes, but neither includes the influence of scattering in its definition. The mean photon path lengths in non-emitting media have been defined [2–4] to incorporate the effects of scattering and absorption into characteristic lengths. These definitions require knowledge of the radiative heat flux and the derivative of the heat flux in the absorbing and scattering (non-emitting) medium and are quite general. However, the reflection/transmission mean photon path length does not characterize medium behavior when volumetric emission is allowed. The mean emission length has been defined to overcome this difficulty [1].

In radiative emission calculations involving real gases, the band models used to describe the gaseous absorption and emission typically require the specification of a path length. With the exception of the photon path length method (described for radiation heat transfer in planar media in ref. [2] and generalized to multidimensional media in ref. [1]), radiative transfer solutions for scattering media do not rigorously incorporate this path length dependence and must approximate the non-gray gas absorption by the definition of mean absorption coefficients for specified spectral intervals. For lack of a better approach, the mean absorption coefficients are usually derived using the mean beam length as the characteristic length scale in the scattering medium. Unfortunately, there is no rigorous basis for this choice. Furthermore, a gray absorption coefficient for a gas which applies over a given spectral interval is an artifice that is not even qualitatively valid in its modeling of gas absorption and emission [5]. The use of the mean absorption coefficient is also questioned by Mengüc and Viskanta [6] in their study of emission from mixtures of gases and particles. Clearly, radiative transfer solutions that account for the influence of scattering and include radiative emission from real gases in a fundamentally correct manner are needed.

This work develops an approach for approximately and accurately computing the radiative emission from multidimensional, homogeneous mixtures of scattering components and real gases. The mean emission length (mean photon path length for volume emission) is identified as a valid characteristic length for such problems, and its use in solving for the energy transfer is described. Examples of the application of this mean emission length method are included with particular emphasis upon its utility in problems involving real gases and scattering particles.

MEAN EMISSION LENGTH ANALYSIS

Initially, the medium is taken to consist of an absorbing, scattering, and emitting constituent that is homogeneous and isothermal with temperature T.

† Present address: New Aircraft Products Division, McDonnell Aircraft Company, P.O. Box 516, St. Louis, MO 63166-0516, U.S.A.

NOMENCLATURE

a	absorption coefficient [m^{-1}]
$\bar{a}_{\Delta\nu g}$	mean gas absorption coefficient for wave number interval $\Delta\nu$ [m^{-1}]
a_ν	spectral absorption coefficient [m^{-1}]
$a_{\nu g}$	secondary spectral absorption coefficient [m^{-1}]
A	area [m^2]
A_i	wide-band absorption for gas band i [cm^{-1}]
A_s	total surface area of the boundary [m^2]
dA	differential area element at which the flux is evaluated [m^2]
dV	differential volume element [m^3]
D	cylinder diameter [m]
F_{bb}	blackbody fraction
i_b	total blackbody intensity [$W\,m^{-2}\,sr^{-1}$]
$i_{\nu b}$	spectral blackbody intensity [$W\,cm\,m^{-2}\,sr^{-1}$]
l	photon path length [m]
$\langle l\rangle_c^{\pm}$	mean emission length at all wave numbers (gray medium) for volume emitted energy arriving at dA [m]
$\langle l\rangle_{\nu e}^{\pm}$	mean emission length at wave number ν for volume emitted energy arriving at dA [m]
L	total layer depth [m]
L_{mb}	surface area average mean beam length, $4V/A_s$ [m]
$L_{mb,l}$	local mean beam length [m]
$\mathbf{n}_{dA}$	normal vector to area element dA
N	number of gas bands
P	phase function
$q_e^{\pm}$	total flux at dA from volume emission [$W\,m^{-2}$]
$q_{\nu e}^{\pm}$	spectral flux at dA from volume emission [$W\,cm\,m^{-2}$]
r	radial coordinate of the cylinder [m]
$\mathbf{r}_{dV}$	location of volume element dV
T	medium temperature [K]
V	total medium volume [m^3]
y	layer coordinate normal to the boundaries [m]
z	axial coordinate of the cylinder [m].

Greek symbols

α_i	gas band intensity [$m^2\,g^{-1}\,cm^{-1}$]
β	extinction coefficient, $(a+\sigma)$ [m^{-1}]
ε	emittance
ε_b	band emittance
η_i	gas band line width to spacing parameter
ν	wave number [cm^{-1}]
ν_c	wave number location of band center for band i [cm^{-1}]
ν_l	lower wave number limit for band i or block k [cm^{-1}]
ν_u	upper wave number limit for band i or block k [cm^{-1}]
ρ	gas density [$kg\,m^{-3}$]
σ	scattering coefficient [m^{-1}]
τ_g	gas transmissivity for band i or block k
τ_{HD}	gas optical depth based upon cylinder diameter, $\alpha_i\rho D/\omega_i$
τ_{Hi}	gas optical depth at band head or center of band i
τ_{HL}	gas optical depth based upon layer depth, $\alpha_i\rho L/\omega_i$
$\Psi^{\pm}(l)$	path length function for volume emission from the entire medium [sr]
$\Psi^{\pm}(l, \mathbf{r}_{dV})$	path length function for volume emission from the element dV [$sr\,m^{-3}$]
ω	scattering albedo, $\sigma/(a+\sigma)$
ω_i	gas band width parameter [cm^{-1}].

Superscripts

+	positive direction
−	negative direction.

Subscripts

$\bar{a}$	mean absorption coefficient value
b	blackbody
c	center
e	emission quantity
exact	exact value
g	real gas property
i	gas band number
k	wave number block number
l	local quantity, lower
l	evaluated at path length l
$\langle l\rangle$	mean emission length value
mb	mean beam length quantity
s	surface quantity
u	upper
ν	wave number dependent quantity
$\Delta\nu$	evaluated at wave number interval $\Delta\nu$.

The boundary is assumed to be transparent, and its shape is arbitrary with the exception that the outer surface cannot view itself. The absorption and scattering within the medium are described by an absorption coefficient a_ν and scattering coefficient σ_ν where ν denotes wave number. The medium phase function is denoted by P_ν. This is the same geometrically general medium shown in ref. [1]. In the next sections, an expression for the emitted flux for this medium is developed and a characteristic length for emission defined. The introduction of a real gas is then addressed using these fundamental analyses.

Radiative heat flux for emission

At an area element dA, either within or on the boundary of the medium, the radiant heat flux resulting from volume emitted energy from all volume elements dV which reaches dA after absorption and scattering in the medium with a transparent boundary is $q_{ve}^{\pm}(T, a_\nu, \sigma_\nu, P_\nu)$. The positive (+) and negative (−) directions are defined relative to a defined normal $\mathbf{n}_{dA}$ at element dA. Note that the entire medium is considered since scattering is a volumetric, rather than line-of-sight, phenomenon. In obtaining an expression for $q_{ve}^{\pm}$, let $\Psi^{\pm}(l, \mathbf{r}_{dV})\,dl$ denote the photon path length probability distribution function for photons with travel lengths between l and $l+dl$, which have been emitted by a volumetric source dV located at $\mathbf{r}_{dV}$ and have arrived at element dA after traversing the conservative medium (the medium with a_ν set to zero). The photon path length distribution function for the entire homogeneous volume $\Psi^{\pm}(l)$ is obtained by integrating over all elemental volumes

$$\Psi^{\pm}(l) = \int_V \Psi^{\pm}(l, \mathbf{r}_{dV})\,dV. \tag{1}$$

The internal volume sources in this case are considered to be diffuse thermal sources of strength $4\pi\,dV$. The flux at dA which results from volume emitted energy that reaches dA in a conservative medium with sources of strength $4\pi a_\nu i_{\nu b}(T)\,dV$ is

$$q_{ve}^{+} = a_\nu i_{\nu b}(T) \int_0^\infty \Psi^{+}(l)\,dl \tag{2}$$

where the quantity $\{a_\nu i_{\nu b}(T)\,\Psi^{\pm}(l)\,dl\}$ represents the contribution to the emitted flux at dA from photons with travel lengths between l and $l+dl$. Introducing absorption, the emitted energy flux is

$$q_{ve}^{\pm} = a_\nu i_{\nu b}(T) \int_0^\infty e^{-a_\nu l}\Psi^{\pm}(l)\,dl. \tag{3}$$

Noting that

$$\frac{\partial(1-e^{-a_\nu l})}{\partial l} = a_\nu e^{-a_\nu l} \tag{4}$$

it is possible to rewrite equation (3) as

$$q_{ve}^{\pm} = i_{\nu b}(T) \int_0^\infty \frac{\partial(1-e^{-a_\nu l})}{\partial l}\Psi^{\pm}(l)\,dl. \tag{5}$$

Integrating equation (5) by parts and noting $\Psi^{\pm}(\infty) = 0$ [1], $q_{ve}^{\pm}$ reduces to

$$q_{ve}^{\pm} = -i_{\nu b}(T) \int_0^\infty (1-e^{-a_\nu l}) \frac{\partial\Psi^{\pm}(l)}{\partial l}\,dl. \tag{6}$$

Finally, with $\Psi^{\pm}(0) = \pi$ [1], equation (6) reduces to

$$q_{ve}^{\pm} = \pi i_{\nu b}(T) + i_{\nu b}(T) \int_0^\infty e^{-a_\nu l} \frac{\partial\Psi^{\pm}(l)}{\partial l}\,dl. \tag{7}$$

This is a general expression for the emitted radiative flux to dA. Although equation (7) can be used directly to solve for the flux, the computations required to define the path length function $\Psi^{\pm}(l)$ are prohibitive for most practical applications. Therefore, in the following sections, an approximate methodology which applies characteristic length scales is developed.

Mean emission length

The integral in equation (7) involves a quantity useful in describing volume emission to the area element dA by the medium. The fact that the integral is over path length with the integrand composed of a probability function leads naturally to the definition of the characteristic mean length for emission using the first moment of the integrand [1]. The mean emission length $\langle l\rangle_{ve}^{\pm}$ is defined as

$$\langle l\rangle_{ve}^{\pm} = \frac{\displaystyle\int_0^\infty l\,e^{-a_\nu l}\frac{\partial\Psi^{\pm}(l)}{\partial l}\,dl}{\displaystyle\int_0^\infty e^{-a_\nu l}\frac{\partial\Psi^{\pm}(l)}{\partial l}\,dl} \tag{8}$$

which describes a characteristic emission length for the volume radiating to dA. This length can also be expressed as

$$\langle l\rangle_{ve}^{\pm} = \frac{-1}{[q_{ve}^{\pm} - \pi i_{\nu b}(T)]}\frac{\partial q_{ve}^{\pm}}{\partial a_\nu} = -\frac{\partial\{\ln[\pi i_{\nu b}(T) - q_{ve}^{\pm}]\}}{\partial a_\nu} \tag{9}$$

which is obtained by rearranging equation (7) and applying the definition of $\langle l\rangle_{ve}^{\pm}$ from equation (8). The general characteristics of this mean emission length are presented in ref. [1], where the behavior of $\langle l\rangle_{ve}^{\pm}$ in various limits and for various geometries is discussed. For example, the value for an area element dA on the boundary of an optically thin medium ($\sigma_\nu \to 0$, $a_\nu \to 0$) is the local value of the mean beam length. It is important to note that using equation (9) to solve for the mean emission length does not require knowledge of the photon path length distribution function. The mean emission length can be evaluated from derivatives of the radiative heat flux with the heat flux determined by any method desired.

Scattering and real gas emission

To complete the development of the computational approach, emission from a more complex medium composed of a mixture of gray scattering constituents and a gaseous absorber is considered. As a first step, a secondary gaseous absorber (no scattering contribution by this component) with absorption coefficient a_{vg} is introduced into the volume. The medium is then taken to be composed of one gray constituent with constant absorption coefficient a, scattering coefficient σ, and phase function P and a gaseous, purely absorbing constituent with spectrally dependent absorption coefficient a_{vg}. In this case, equation (6) can be rearranged to yield ($a_\nu = a + a_{vg}$)

$$q_{ve}^{\pm} = q_{ve}^{\pm}(a_{vg}=0) - i_{vb}(T) \times \int_0^{\infty} [1-e^{-a_{vg}l}]\, e^{-al} \frac{\partial \Psi^{\pm}(l)}{\partial l}\, dl \quad (10)$$

where $q_{ve}^{\pm}(a_{vg}=0)$ is the contribution for the medium without a real gas component. If the secondary constituent is a real gas such as CO_2 or H_2O and the gas absorption is modeled with the exponential wide-band model [5], integration over wave number introduces the wide-band absorption A_i, defined as

$$A_i = \int_{\text{band } i} [1-e^{-a_{vg}l}]\, d|\nu - \nu_i|. \quad (11)$$

For a gas with a single wide band, equation (10) then becomes

$$q_e^{\pm} = q_e^{\pm}(a_{vg}=0) - \int_0^{\infty} [i_{\nu_i b}(T) A_i(l)] e^{-al} \frac{\partial \Psi^{\pm}(l)}{\partial l}\, dl \quad (12)$$

where only the functional dependence of A_i on path length is explicitly denoted. In the weak band (optically thin gas) limit, A_i is a linear function of path length l

$$A_i(l) = \omega_i \tau_{Hli} = \omega_i \left(\frac{\alpha_i \rho l}{\omega_i}\right) = \alpha_i \rho l. \quad (13)$$

In equation (13), τ_{Hli} is the gas optical depth at band head or center evaluated with length l, α_i the band intensity, ω_i the band width parameter, and ρ the gas density. Introducing equation (13) into equation (12) and applying the definition of the mean emission length $\langle l \rangle_e^{\pm}$, the optically thin gas limit is obtained as

$$q_e^{\pm} = q_e^{\pm}(a_{vg}=0) - \int_0^{\infty} [i_{\nu_i b}(T) \alpha_i \rho l]\, e^{-al} \frac{\partial \Psi^{\pm}(l)}{\partial l}\, dl \quad (14)$$

or

$$q_e^{\pm} = q_e^{\pm}(a_{vg}=0) - \frac{i_{\nu_i b}(T)}{i_b(T)} \alpha_i \rho \langle l \rangle_e^{\pm} \times [q_e^{\pm}(a_{vg}=0) - \pi i_b(T)]. \quad (15)$$

Replacing $\alpha_i \rho \langle l \rangle_e^{\pm}$ by $A_i(\langle l \rangle_e^{\pm})$, which is strictly valid in the optically thin gas limit, equation (15) reduces to

$$q_e^{\pm} = q_e^{\pm}(a_{vg}=0) - \frac{i_{\nu_i b}(T)}{i_b(T)} A_i(\langle l \rangle_e^{\pm}) \times [q_e^{\pm}(a_{vg}=0) - \pi i_b(T)]. \quad (16)$$

For a gas with many bands, equation (16) is easily extended as

$$q_e^{\pm} = q_e^{\pm}(a_{vg}=0) - \left[\sum_i \frac{i_{\nu_i b}(T)}{i_b(T)} A_i(\langle l \rangle_e^{\pm})\right] \times [q_e^{\pm}(a_{vg}=0) - \pi i_b(T)]. \quad (17)$$

If band overlap exists, the block transmissivity form of the wide-band gas modeling is desirable [5]. Equation (16) for a single band i is

$$q_e^{\pm} = q_e^{\pm}(a_{vg}=0) - \{[1-\tau_{gi}(\langle l \rangle_e^{\pm})] F_{bb}(\nu_{li}(\langle l \rangle_e^{\pm}), \nu_{ui}(\langle l \rangle_e^{\pm}), T)\} [q_e^{\pm}(a_{vg}=0) - \pi i_b(T)] \quad (18)$$

and equation (17) for multiple bands is

$$q_e^{\pm} = q_e^{\pm}(a_{vg}=0) - \left\{\sum_k [1-\tau_{gk}(\langle l \rangle_e^{\pm})] F_{bb}(\nu_{lk}(\langle l \rangle_e^{\pm}), \nu_{uk}(\langle l \rangle_e^{\pm}), T)\right\} [q_e^{\pm}(a_{vg}=0) - \pi i_b(T)]. \quad (19)$$

In equations (18) and (19), ν_l and ν_u are the lower and upper wave number bounds for band i or spectral block k, F_{bb} the blackbody fraction, and τ_g the block transmissivity of the gas within band i or spectral block k.

The advantage of equations (16)–(19) is that $q_e^{\pm}(a_{vg}>0)$ is calculated very easily for an optically thin real gas using only $q_e^{\pm}(a_{vg}=0)$ and $\langle l \rangle_e^{\pm}$, defined for the gray-constituent medium. For fixed values of the scattering coefficient σ, absorption coefficient a, and phase function P, which describe the gray constituent, the flux $q_e^{\pm}(a_{vg}>0)$ may be calculated approximately for any desired condition of the gaseous constituent(s). That is, with the gray constituent fixed, $q_e^{\pm}(a_{vg}=0)$ and $\langle l \rangle_e^{\pm}$ are also fixed, and the only variables in equations (16)–(19) are the gas band absorption quantities, evaluated with length $\langle l \rangle_e^{\pm}$.

If a second-order finite difference approximation is used in calculating the derivative in equation (9), at the most three calculations of the gray medium flux (e.g. $q_e^{\pm}(a,\ a_{vg}=0)$, $q_e^{\pm}(a+\Delta a,\ a_{vg}=0)$, and $q_e^{\pm}(a-\Delta a,\ a_{vg}=0)$) are necessary to define $q_e^{\pm}(a_{vg}=0)$ and $\langle l \rangle_e^{\pm}$. By contrast, conventional methods of solving for the flux $q_e^{\pm}(a_{vg}>0)$ require the definition of mean gas absorption coefficients $\bar{a}_{\Delta \nu_i g}$ for each band using the mean beam length as the radiative length scale. The complete solution for a problem with N bands then requires $N+1$ flux calculations (one for each ith band with absorption coefficient $(a+\bar{a}_{\Delta \nu_i g})$ and one for the spectral regions outside the bands with absorption coefficient a). The mean emission length approach requires only three flux calculations, regardless of the number of bands, and therefore provides a significant computational advantage. Furthermore, the application of the mean gas absorption coefficients is an uncertain process, as noted in the Introduction.

Also, note that even though the formulation above is presented in terms of the wide-band model for gaseous absorption and emission, narrow-band gas models present no added complexity. The effective bandwidth of a narrow band is a linear function of path length in the optically thin gas limit, just as for a wide band. Thus, with a slight change in notation, the formulations given above are easily generalized to incorporate narrow-band gas modeling. In this case, the computational advantage of the mean emission

length approach is even greater. For example, with the hundreds of narrow bands that may require consideration for a mixture of gases and gray particles, the mean emission length approach still requires only three evaluations of the medium flux, in contrast to the mean absorption coefficient approach which requires $N+1$ flux calculations (for N narrow bands).

For a medium with a non-gray particulate, the radiative properties of the particles can generally be approximated as gray over spectral intervals that are large compared to the extent of gas bands. In this situation, the mean emission length approach requires three flux calculations for each spectral interval over which the particulate is considered gray and retains its computational advantage as long as the number of gas bands within each gray-particle spectral interval is greater than two.

The utility of this mean emission length formulation would indeed be limited if only an optically thin gas were treatable. As will be demonstrated below, equations (16)–(19) provide reasonably accurate solutions for the flux $q_e^{\pm}$, even when the gas is optically thick. This flexibility was previously noted in ref. [2] for reflection and transmission problems involving scattering media with real gases.

RESULTS

In order to demonstrate the use and accuracy of equations (16)–(19), the radiant flux is computed at the boundary of media containing isotropically scattering gray particles (characterized by a, σ, and $P = 1$) and a real gas with a single wide band i. So that the accuracy of the mean emission length approach may be judged, exact flux values are also calculated. Finally, to demonstrate the relative accuracy of the approximate mean absorption coefficient approach, flux calculations obtained via this method are also given.

Band emittance expressions

An approximate comparison between these three sets of results which isolates that element of the flux calculation that is most sensitive to the modeling differences is based on a band emittance quantity ε_b for a boundary element dA. This band emittance is plotted in the figures which follow and is defined as

$$\varepsilon_b = \frac{q_e^+ - q_e^+(a_{vg}=0)}{\pi i_b(T)}. \tag{20}$$

The positive (+) normal vector at dA is directed out of the medium. Because the mean absorption coefficient approach requires the construction of a gray band with well-defined wave number bounds, the block transmissivity form of the wide-band gas modeling is employed. For a single wide band i, the exact band emittance is developed from equation (10) using a procedure similar to that used in developing the mean emission length result in equation (18). This yields

$$\varepsilon_{b,\text{exact}} = \frac{-1}{\pi}\int_0^\infty \{[1-\tau_{gi}(l)]F_{bb}(\nu_{li}(l),\nu_{ui}(l),T)\} \times e^{-al}\frac{\partial\Psi^+(l)}{\partial l}\,dl. \tag{21}$$

This equation is solved by numerically simulating the photon path length function $-\partial\Psi^+(l)/\partial l$ using Monte Carlo in the conservative medium with a transparent boundary [1].

The comparable mean emission length result is obtained from equation (18) as

$$\varepsilon_{b,\langle l\rangle} = -\{[1-\tau_{gi}(\langle l\rangle_e^+)] \times F_{bb}(\nu_{li}(\langle l\rangle_e^+),\nu_{ui}(\langle l\rangle_e^+),T)\} \times [q_e^+(a_{vg}=0)-\pi i_b(T)]\frac{1}{\pi i_b(T)} \tag{22}$$

or

$$\varepsilon_{b,\langle l\rangle} = -\{[1-\tau_{gi}(\langle l\rangle_e^+)] \times F_{bb}(\nu_{li}(\langle l\rangle_e^+),\nu_{ui}(\langle l\rangle_e^+),T)\}[\varepsilon(a)-1] \tag{23}$$

where $\varepsilon(a)$ is the gray-medium emittance (not band emittance) for absorption coefficient a, scattering coefficient σ, and phase function P

$$\varepsilon(a) = \frac{q_e^+(a_{vg}=0)}{\pi i_b(T)}. \tag{24}$$

The comparable mean absorption coefficient result is obtained by spectrally integrating equation (10) to obtain the total emitted flux q_e^+ at a boundary location dA. However, rather than introduce the wide-band absorption A_i for the gas band, an approximate mean absorption coefficient $\bar{a}_{\Delta\nu_i g}$ is defined for the spectral band, ν_{li} to ν_{ui}, as

$$q_e^+ = q_e^+(a_{vg}=0) - \int_0^\infty\left[\int_{\nu_{li}}^{\nu_{ui}} i_{\nu b}(T) \times (1-e^{-\bar{a}_{\Delta\nu_i g}l})\,d\nu\right]e^{-al}\frac{\partial\Psi^+(l)}{\partial l}\,dl. \tag{25}$$

The band emittance $\varepsilon_{b,\bar{a}}$, obtained using the mean absorption coefficient, is then

$$\varepsilon_{b,\bar{a}} = \frac{q_e^+ - q_e^+(a_{vg}=0)}{\pi i_b(T)} = \frac{-1}{\pi} \times \int_0^\infty\left[\int_{\nu_{li}}^{\nu_{ui}}\frac{i_{\nu b}(T)}{i_b(T)}(1-e^{-\bar{a}_{\Delta\nu_i g}l})\,d\nu\right]e^{-al}\frac{\partial\Psi^+(l)}{\partial l}\,dl. \tag{26}$$

Since $\bar{a}_{\Delta\nu_i g}$ is constant, the factor $(1-e^{-\bar{a}_{\Delta\nu_i g}l})$ can be removed from the spectral integration, giving

$$\varepsilon_{b,\bar{a}} = F_{bb}(\nu_{li},\nu_{ui},T)\left(\frac{-1}{\pi}\right) \times \int_0^\infty (1-e^{-\bar{a}_{\Delta\nu_i g}l})\,e^{-al}\frac{\partial\Psi^+(l)}{\partial l}\,dl \tag{27}$$

or

$$\varepsilon_{b,\bar{a}} = F_{bb}(\nu_{li}, \nu_{ui}, T)\left[\frac{-1}{\pi}\int_0^\infty e^{-al}\frac{\partial\Psi^+(l)}{\partial l}\,dl + \frac{1}{\pi}\int_0^\infty e^{-(\bar{a}_{\Delta\nu_i g}+a)l}\frac{\partial\Psi^+(l)}{\partial l}\,dl\right]. \quad (28)$$

Considering equation (7) and equation (24), note that the emittance (not band emittance) of a gray medium with absorption coefficient a can be written as

$$\varepsilon(a) = \frac{q_e^+}{\pi i_b(T)} = 1 + \frac{1}{\pi}\int_0^\infty e^{-al}\frac{\partial\Psi^+(l)}{\partial l}\,dl. \quad (29)$$

Then, adding and subtracting unity within the brackets in equation (28) yields

$$\varepsilon_{b,\bar{a}} = F_{bb}(\nu_{li}, \nu_{ui}, T) \times\left\{-\left[1+\frac{1}{\pi}\int_0^\infty e^{-al}\frac{\partial\Psi^+(l)}{\partial l}\,dl\right] + \left[1+\frac{1}{\pi}\int_0^\infty e^{-(\bar{a}_{\Delta\nu_i g}+a)l}\frac{\partial\Psi^+(l)}{\partial l}\,dl\right]\right\} \quad (30)$$

or

$$\varepsilon_{b,\bar{a}} = F_{bb}(\nu_{li}, \nu_{ui}, T)[\varepsilon(a+\bar{a}_{\Delta\nu_i g}) - \varepsilon(a)] \quad (31)$$

where $\varepsilon(a)$ is defined by equation (29) and $\varepsilon(a+\bar{a}_{\Delta\nu_i g})$ is the gray medium emittance for absorption coefficient $(a+\bar{a}_{\Delta\nu_i g})$. The remaining medium properties, scattering coefficient σ and phase function P, are unchanged.

Equation (31) is therefore used to evaluate the band emittance under the approximation of the mean absorption coefficient. However, $\bar{a}_{\Delta\nu_i g}$, ν_{li}, and ν_{ui} must first be properly defined for gas band i. To ensure the greatest measure of consistency between this calculation and that of the mean emission length, the block transmissivity form of the wide-band gas modeling [5] is applied. To define $\bar{a}_{\Delta\nu_i g}$, the block (or band) transmissivity τ_{gi} for block i is evaluated using Edwards' relations with the corrected mean beam length $(0.9L_{mb})$ used as the medium length scale (i.e. with τ_{H_i} as the gas optical depth at band head or center for band i evaluated with length $0.9\,L_{mb}$). $\bar{a}_{\Delta\nu_i g}$ is then approximated by writing τ_{gi} as

$$\tau_{gi} = \exp(-\bar{a}_{\Delta\nu_i g} 0.9\,L_{mb}). \quad (32)$$

Thus, $\bar{a}_{\Delta\nu_i g}$ is calculated as

$$\bar{a}_{\Delta\nu_i g} = \frac{-1}{0.9\,L_{mb}}\ln(\tau_{gi}). \quad (33)$$

The block or band limits, ν_{li} and ν_{ui}, are computed using the appropriate expressions from Edwards for a centered band at ν_{ci}, where the wave number interval $\Delta\nu_i$ also incorporates 0.9 L_{mb} as the characteristic length scale. Thus, the quantities needed for the evaluation of the band emittance in equation (31) are defined.

Comparisons

Equations (21), (23), and (31) define the band emittance ε_b for the three approaches: exact, mean emission length, and mean absorption coefficient. In the results to follow, $\varepsilon_{b,exact}$ is computed by numerically simulating the photon path length function $-\partial\Psi^+(l)/\partial l$ via Monte Carlo. $\varepsilon_{b,\langle l\rangle}$ and $\varepsilon_{b,\bar{a}}$ require calculations of the emittance ε of a gray medium; $\varepsilon_{b,\bar{a}}$ requires $\varepsilon(a)$ and $\varepsilon(a+\bar{a}_{\Delta\nu_i g})$ while $\varepsilon_{b,\langle l\rangle}$ requires $\varepsilon(a)$, at least. $\varepsilon_{b,\langle l\rangle}$ also needs the mean emission length $\langle l\rangle_e^+$, which could be defined using $\varepsilon(a+\Delta a)$ and $\varepsilon(a-\Delta a)$ as part of a finite difference approximation to the derivative in equation (9). Instead, since the exact solution produces the path length function $-\partial\Psi^+(l)/\partial l$ directly, $\langle l\rangle_e^+$ is computed using the integral expression of equation (8) and is defined for the gray medium with properties a, σ, and P.

With $\varepsilon_{b,exact}$, $\varepsilon_{b,\langle l\rangle}$, and $\varepsilon_{b,\bar{a}}$ described, representative calculations for planar and cylindrical media with transparent boundaries are provided in Figs. 1–7. As stated previously, the constituents are an isotropically scattering gray particulate (a, σ, $P = 1$) and a real gas with a single wide band. The band width parameter ω_i is fixed at 50 cm^{-1}, the line width to spacing parameter η_i is fixed at 2, the temperature is 1000 K, the total pressure is 1 atm, and the gas band is the 2.7 μm CO_2 band. Results for the layer are given in Figs. 1 and 2, where ε_b is plotted vs layer gas optical depth τ_{H_L}; results for the cylinder with aspect ratio $L/D = 3$

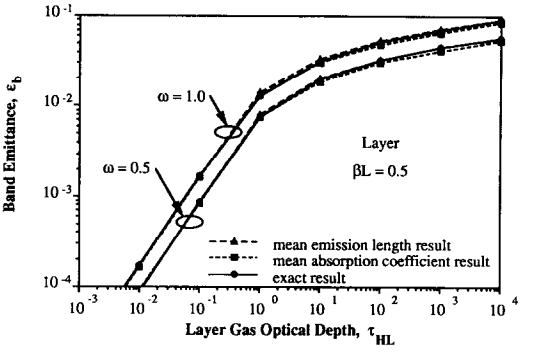

FIG. 1. Comparison of band emittances for a layer with particle optical depth $\beta L = 0.5$.

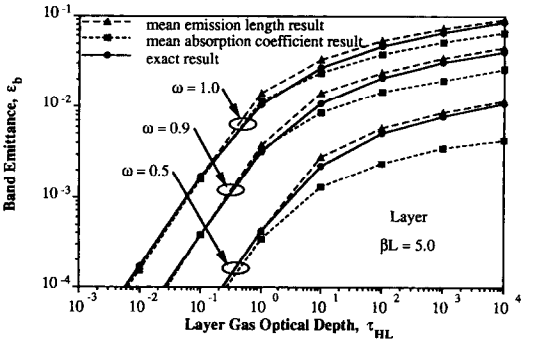

FIG. 2. Comparison of band emittances for a layer with particle optical depth $\beta L = 5.0$.

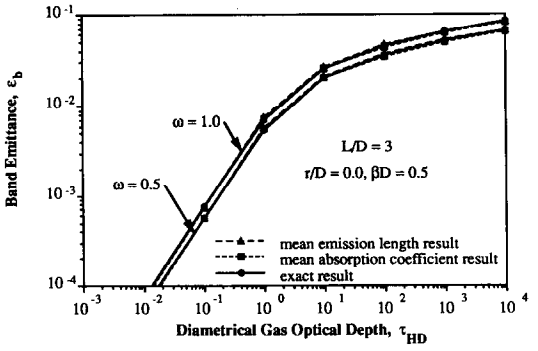

FIG. 3(a). Comparison of band emittances at radial location $r/D = 0.0$ of a cylinder (aspect ratio $L/D = 3$) with particle optical depth $\beta D = 0.5$.

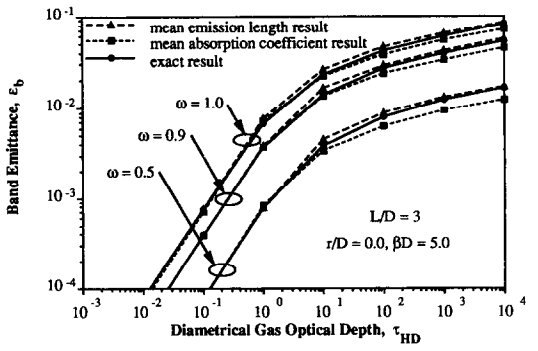

FIG. 4(a). Comparison of band emittances at radial location $r/D = 0.0$ of a cylinder (aspect ratio $L/D = 3$) with particle optical depth $\beta D = 5.0$.

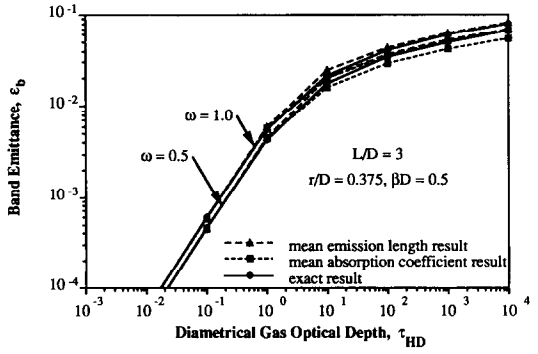

FIG. 3(b). Comparison of band emittances at radial location $r/D = 0.375$ of a cylinder (aspect ratio $L/D = 3$) with particle optical depth $\beta D = 0.5$.

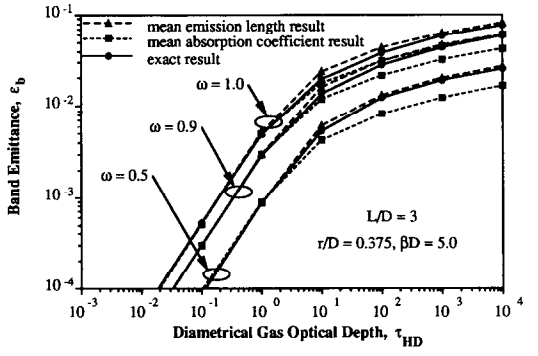

FIG. 4(b). Comparison of band emittances at radial location $r/D = 0.375$ of a cylinder (aspect ratio $L/D = 3$) with particle optical depth $\beta D = 5.0$.

(L is the axial length and D the diameter) are given in Figs. 3–7, where ε_b is plotted vs diametrical gas optical depth τ_{HD}. The particle properties investigated are extinction optical depths βL of 0.5 and 5.0 for the layer and βD of 0.5 and 5.0 for the cylinder. The scattering albedo ω is fixed at 0.5, 0.9, and 1.0; in some cases, the $\omega = 0.9$ data is disregarded since its inclusion would make the plotted lines indistinguishable.

In each figure, a single value of particle optical depth is investigated, and the plotted values of $\varepsilon_{b,exact}$, $\varepsilon_{b,\langle l\rangle}$, and $\varepsilon_{b,\bar{a}}$ generally group together for each value of albedo. Figures 1 and 2 are plots of band emittance for the layer with particle extinction optical depths of 0.5 and 5.0, respectively. Figures 3–6 each involve a pair of figures which compare 'corner' and 'center' locations on the $L/D = 3$ cylinder for a single value of particle optical depth. Corner locations are taken to mean the locations $r/D = 0.375$ and $z/D = 0.05$ while center locations are $r/D = 0.0$ (the base center) and $z/D = 1.5$ (the side center). Each of Figs. 3–6 then compares either the base corner to base center or side corner to side center for a particular value of particle optical depth. Figure 7 is a plot of band emittance for a particle optical depth of 5.0 and a location $z/D = 0.375$ on the cylinder's side (between $z/D =$ 0.05 and 1.5).

For each plotted value of ε_b, the Monte Carlo solutions for $\varepsilon_{b,exact}$, $\varepsilon(a)$, $\varepsilon(a+\bar{a}_{\Delta\nu g})$, and $\langle l\rangle_c^+$ each entailed five iterations of 10 000 bundles. As a general rule, the 99% confidence intervals for the computed quantities are less than about $\pm 4.25\%$ of the computed average values, in the worst case, and are typically less than $\pm 1\%$.

Considering Figs. 1–7, it is apparent that the general trend is for the mean emission length approach to provide better accuracy than the mean absorption coefficient method at both small (linear gas absorption regime) and large (logarithmic gas absorption regime) gas optical depths. In fact, in the limit of τ_{HL} or τ_{HD} approaching zero, the mean emission length results are exact. At intermediate values of gas optical depth (approximately 1–10), the two approaches are of comparable accuracy—the mean emission length result is generally more accurate yet the mean absorption coefficient result is more accurate in some instances.

Other trends are also apparent. Greater differences between $\varepsilon_{b,\langle l\rangle}$ and $\varepsilon_{b,\bar{a}}$ generally occur as βL or βD increases (compare βL or $\beta D = 0.5$ results to those of βL or $\beta D = 5.0$ for each location) and as ω decreases, with the mean emission length results typically being more accurate. Also, comparing the band emittances $\varepsilon_{b,\langle l\rangle}$ and $\varepsilon_{b,\bar{a}}$ for corner and center locations for a single value of particle optical depth (i.e. compare Fig.

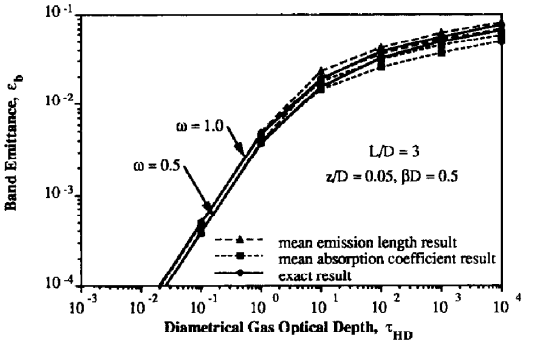

FIG. 5(a). Comparison of band emittances at axial location $z/D = 0.05$ of a cylinder (aspect ratio $L/D = 3$) with particle optical depth $\beta D = 0.5$.

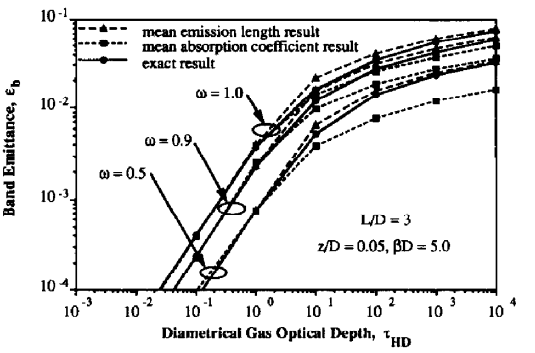

FIG. 6(a). Comparison of band emittances at axial location $z/D = 0.05$ of a cylinder (aspect ratio $L/D = 3$) with particle optical depth $\beta D = 5.0$.

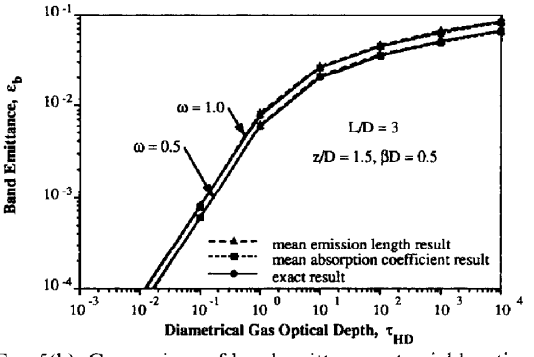

FIG. 5(b). Comparison of band emittances at axial location $z/D = 1.5$ of a cylinder (aspect ratio $L/D = 3$) with particle optical depth $\beta D = 0.5$.

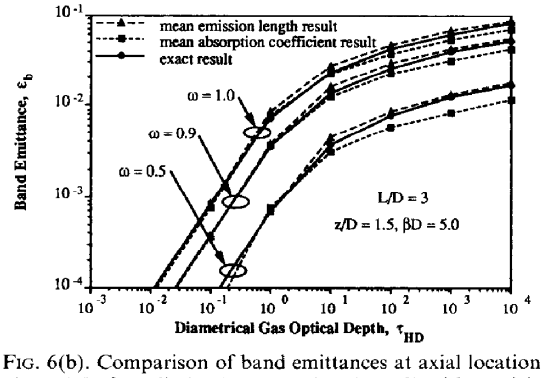

FIG. 6(b). Comparison of band emittances at axial location $z/D = 1.5$ of a cylinder (aspect ratio $L/D = 3$) with particle optical depth $\beta D = 5.0$.

3(a) to 3(b), 4(a) to 4(b), etc.) greater differences clearly exist in the corners. These trends are explainable considering the values of the mean emission length in these instances. The plotted values of $\langle l \rangle_e^+ / L_{mb}$ for the $L/D = 3$ cylinder in ref. [1] demonstrate analogous trends. That is, the differences between $\langle l \rangle_e^+$ and L_{mb} are most evident as βD becomes large, as ω becomes small, and as the corner of the cylinder is approached. This demonstrates that the effect of the participating medium and the multidimensional nature of the energy transfer to the cylinder's boundary are of paramount importance in determining the proper characteristic length in the medium. Therefore, the mean absorption coefficient approach, which uses L_{mb} as the medium's length scale, predicts the band emittance ε_b poorly under precisely those conditions where $\langle l \rangle_e^+$ and L_{mb} differ the most. Figure 7, which applies for an intermediate location ($z/D = 0.375$) on the cylinder's side, shows trends very similar to those in Fig. 6(b), which applies for the same particle optical depth ($\beta D = 5.0$) but at the side center location ($z/D = 1.5$). Analogously, the values of $\langle l \rangle_e^+ / L_{mb}$ from ref. [1] at these locations are not significantly different for $\beta D = 5.0$, at least for $\omega = 0.5$ and 0.9. Thus, the fact that the characteristic length $\langle l \rangle_e^+$ changes little between the two locations is reflected in the similarity of the band emittance results.

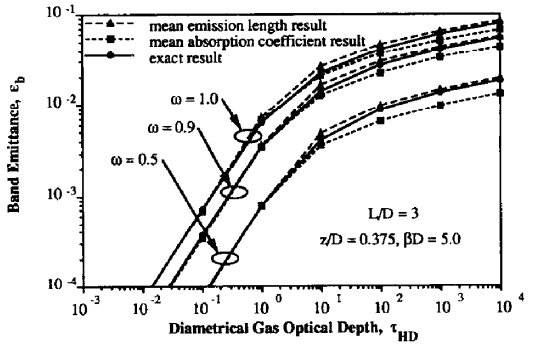

FIG. 7. Comparison of band emittances at axial location $z/D = 0.375$ of a cylinder (aspect ratio $L/D = 3$) with particle optical depth $\beta D = 5.0$.

All of the plotted results are for fixed values of the band parameters η_i and ω_i ($\eta_i = 2$, $\omega_i = 50$ cm^{-1}), fixed temperature ($T = 1000$ K), fixed band position (2.7 μm CO_2 band), and fixed cylinder aspect ratio ($L/D = 3$). In order to test if the trends noted in discussing Figs. 1–7 are extendable to other medium conditions, further comparisons between $\varepsilon_{b,exact}$, $\varepsilon_{b,\langle l \rangle}$, and $\varepsilon_{b,\bar{a}}$ were performed for varying values of η_i, ω_i, T, band position, and cylinder aspect ratio. For all cases tested, the trend of $\varepsilon_{b,\langle l \rangle}$ being more accurate at

both small and large gas optical depth τ_{HD} remained valid. At intermediate values of τ_{HD}, $\varepsilon_{b,\langle l\rangle}$ and $\varepsilon_{b,\bar{a}}$ were again of comparable accuracy, with the mean emission length approach showing its greatest percent error in this region.

CONCLUSIONS

A photon path length formulation has been presented for the evaluation of the emitted flux to an area element within or on the boundary of an arbitrarily shaped, homogeneous, absorbing, emitting, and scattering medium. With this formulation and the introduction of the mean emission length (a meaningful characteristic length for emission in a scattering medium), an approximate yet accurate approach for computing the emission from a medium containing scattering particles and a real gas is developed. Although the photon path length approach is used in the formulation, the resulting method may be used without knowledge of the path length distribution function. An example of how the mean emission length approach may be applied to radiation problems with a generic secondary absorber is provided, along with specific calculations for emission from scattering media containing a real gas. It is shown that the mean emission length constitutes a radiative length scale that is applicable over a wide range of gas optical depths. The mean emission length approach to radiative emission calculations involving real gases generally provides superior accuracy and computational efficiency, compared to results obtained using mean gas absorption coefficients.

REFERENCES

1. D. V. Walters and R. O. Buckius, On the characteristic lengths for absorbing, emitting, and scattering media, *Int. J. Heat Mass Transfer* **33**, 805–813 (1990).
2. R. O. Buckius, Radiation heat transfer using mean photon path lengths, *Int. J. Heat Mass Transfer* **25**, 917–923 (1982).
3. R. D. Skocypec and R. O. Buckius, Photon path length distributions for an isotropically scattering planar medium, *J. Quant. Spectrosc. Radiat. Transfer* **28**, 425–439 (1982).
4. W. M. Irvine, The formation of absorption bands and the distribution of photon optical paths in a scattering atmosphere, *Bull. Astron. Inst. Neth.* **17**(4), 266–279 (1964).
5. D. K. Edwards, Molecular gas band radiation. In *Advances in Heat Transfer* (Edited by T. F. Irvine and J. P. Hartnett), Vol. 12, pp. 115–193. Academic Press, New York (1976).
6. M. P. Mengüc and R. Viskanta, An assessment of spectral radiative heat transfer predictions for a pulverized coal-fired furnace, *Heat Transfer 1986, Proc. Eighth Int. Heat Transfer Conf.*, San Francisco, California, Vol. 2, pp. 815–820 (1986).

APPROCHE PAR LA LONGUEUR D'EMISSION MOYENNE POUR LE TRANSFERT RADIATIF AVEC DIFFUSION ET ABSORPTION DES GAZ REELS

Résumé—On présente une approche numérique de l'analyse de l'émission radiative pour les applications où les milieux multidimensionnels, absorbants, émettants et diffusants sont importants et où les contributions des gaz réels peuvent être incluses. La méthode de la longueur d'émission moyenne est développée pour résoudre le transfert d'énergie, comme étant une approche précise de ces problèmes. Bien qu'utilisant la méthode de la longueur de parcours du photon, l'analyse choisie ne nécéssite pas la connaissance des fonctions de distribution des longueurs de parcours des photons. Des exemples d'application de cette approche pour l'émission sont inclus avec une attention particulière sur son utilité dans les problèmes concernant les gaz réels et les particules diffusantes. Des résultats numériques pour des milieux plans et cylindriques et plusieurs domaines d'épaisseurs optiques et d'albedos sont présentés et la précision élevée et l'efficacité des calculs de cette méthode comparées à celles d'autres approches connues sont démontrées.

ANWENDUNG DES VERFAHRENS DER MITTLEREN EMISSIONSLÄNGE AUF DEN MEHRDIMENSIONALEN STRAHLUNGSAUSTAUSCH UNTER BERÜCKSICHTIGUNG VON STREUUNG UND ABSORPTION IM REALEN GAS

Zusammenfassung—Die Emission von Strahlung wird mit Rechnerunterstützung für mehrdimensionale absorbierende emittierende und streuende Medien für solche Fälle untersucht, bei denen die Realgas-Beiträge berücksichtigt werden müssen. Es wird ein Verfahren zur Lösung des Energietransport-Problems aufgrund mittlerer Emissionslängen entwickelt, das eine Näherungsmethode für solche Probleme darstellt und trotzdem genau ist. Obwohl das Verfahren unter Verwendung der Photonenpfadlängen-Methode entwickelt wurde, ist für die daraus folgende Analyse keine Kenntnis der Verteilungsfunktion der Photonenpfadlänge erforderlich. Es werden Beispiele für die Anwendung dieses Ansatzes für die Emission vorgestellt, wobei besonderer Wert auf seine Nützlichkeit bei der Lösung von Problemen mit realen Gasen und streuenden Partikeln gelegt wird. Numerische Ergebnisse für ebene und zylindrisch angeordnete Medien werden in einem Bereich der optischen Dicke und des Streualbedo vorgestellt. Dabei wird insbesondere die hohe Genauigkeit und die Effizienz der Berechnungen mit diesem Verfahren im Vergleich zu anderen üblichen Rechenmethoden demonstriert.

ИСПОЛЬЗОВАНИЕ МЕТОДА СРЕДНЕЙ ДЛИНЫ ИЗЛУЧЕНИЯ ДЛЯ ОПРЕДЕЛЕНИЯ МНОГОМЕРНОГО ЛУЧИСТОГО ПЕРЕНОСА С УЧЕТОМ РАССЕЯНИЯ И ПОГЛОЩЕНИЯ РЕАЛЬНОГО ГАЗА

Аннотация—Представлен метод расчета процесса излучения в многомерных поглощающих, излучающих и рассеивающих средах с учетом свойств реального газа. Разработан приближенный, но достаточно точный метод средней длины излучения для решения задачи переноса энергии. Несмотря на то, что анализ основан на методе длины пробега фотона, для него не требуется знания функций распределения этой длины. Даются примеры использования предложенного подхода к определению излучения, причем особое внимание уделяется задачам, включающим реальные газы и рассеивающие частицы. Представлены численные результаты для сред плоских и цилиндрических объемов в исследуемых диапазонах оптической глубины и альбедо рассеяния, и продемонстрирована более высокая точность и эффективность расчетов с использованием предложенного метода по сравнению с другими подходами.